COMPDYN 2013
4th ECCOMAS Thematic Conference on
Computational Methods in Structural Dynamics and Earthquake Engineering
M. Papadrakakis, V. Papadopoulos, V. Plevris (eds.)
Kos Island, Greece, 12–14 June 2013

SYSTEM RELIABILITY ANALYSIS OF SLENDER NETWORK ARCH BRIDGES

Anders Rønnquist[1] **and Arvid Naess**[2]

[1] Department of Structural Engineering
Norwegian University of Science and Technology
NO-7491 Trondheim, Norway
e-mail: anders.ronnquist@ntnu.no

[2] Centre for Ships and Ocean Structures & Department of Mathematical Sciences
Norwegian University of Science and Technology
NO-7491 Trondheim, Norway
e-mail: arvid.naess@ntnu.no

Keywords: System reliability, Network Arch Bridges, Monte Carlo Simulation

Abstract. *In principle, the reliability of complex structural systems can be accurately predicted through Monte Carlo simulation. This method has several attractive features for structural system reliability, the most important being that the system failure criterion is usually relatively easy to check almost irrespective of the complexity of the system. However, the computational cost involved in the simulation may be prohibitive for highly reliable structural systems. Network arched bridges are in their design slender structures which by their efficient configuration can carry loads several times higher than for more traditional tie arched bridges with vertical hangers. These bridges are seen as an attractive structure due to their slenderness which also might make them vulnerable to global system buckling. The buckling reliability of network arch bridges are therefore investigated with emphasis on geometric uncertainties*

1 INTRODUCTION

In recent years, the structural assessments of new and existing structures have included probabilistic methods to get a broader insight into the structural behavior over time. Reliability tools have been shown to be a valuable contribution in the decision making process. For all structures, either already existing or to be built and perhaps especially for large civil engineering structures, these tools can be used to evaluate different alternative methods and scenarios, see e.g. [3].

The improvement of the structural understanding during the life span of large infrastructures has at the present time become an important problem to be addressed. This is partly due to the situation of an ever increasing number of infrastructures reaching their final stage of design life, and partly due to changing loads and nonfulfillment of maintenance, rendering physical signs of wear and tear. Results from these observations will ultimately lead to some major decisions for the elected politicians to make regarding our existing and future infrastructure. Should it be invested in upgrading to achieve an extended service life or rather replace dilapidated structures with new? Both of these alternatives will demand major investments in the immediate future to uphold today's standard and to include future demands.

The solution of realistic structural system reliability problems is generally exceedingly difficult to obtain through conventional reliability methods such as the FORM/SORM methods. The main reason is the high number of limit state functions and basic random variables that may be required to define the problem. The system failure event in a realistic case may be defined by a complex combination of failure modes, in general as a combination of series and parallel systems. The failure criteria are very often associated with nonlinear structural behavior, requiring computationally demanding numerical approaches such as the nonlinear FE analysis to accurately assess the structural capacity.

At least in principle, the reliability of complex structural systems can be accurately predicted through Monte Carlo simulation. With this method the system failure criterion is relatively easy to evaluate almost irrespective of the complexity of the system and the number of basic random variables. However, the system failure probabilities are typically of rather small magnitude and therefore the computational cost involved in the Monte Carlo simulation may be prohibitive. If numerical approaches are used to assess the structural capacity, the problem may be intractable if efficient techniques such as the response surface method were not used.

A new Monte Carlo based method for system reliability estimation that aims to reduce the computational cost was recently proposed in [12]. It exploits the regularity of tail probabilities to set up an approximation procedure for the prediction of the far tail failure probabilities based on the estimates obtained by Monte Carlo simulations at more moderate levels. The method was first applied in [12] to small structural systems and later in [13] to a complex system involving a high number of limit state functions and basic random variables. It was shown that the method provides good estimates for the system failure probability with low to moderate computational cost. In this study the method is used to estimate the global system buckling of a network arch bridge represented by a FE structural model.

2 EFFICIENT SYSTEM RELIABILITY ESTIMATION

Consider a structural system for which several failure modes may be defined, and assume that each failure mode is represented by a safety margin,

$$M_i = G_i\left(X_1, \cdots, X_n\right) \tag{1}$$

with G_i, i = 1, …, m, the limit state function that defines the safety margin M_i as a function of a vector $X = [X_1, \ldots, X_n]^T$ of n basic random variables. The limit state function G_i can be a ra-

ther complicated function of the random vector X. In many cases a closed-form equation is not known and the evaluation of G_i requires computationally demanding numerical models, e.g., non-linear FE-models. Failure in mode i of the system is assumed to occur when $M_i = G_i(X) \leq 0$. For a basic system of m failure modes in series the system failure probability is defined by,

$$p_f = \mathrm{P}\left[\bigcup_{i=1}^{m}\left(M_i \leq 0\right)\right] \tag{2}$$

while for the parallel case it is,

$$p_f = \mathrm{P}\left[\bigcap_{i=1}^{m}\left(M_i \leq 0\right)\right]. \tag{3}$$

These are the elementary cases considered in structural systems reliability analysis [9], which are here introduced as example.

To overcome the computational cost typically involved in the estimation of the failure probability of a system of failure modes, the method proposed in [12] formulates the system safety margins in the following way:

$$M_i(\lambda) = M_i - \mu_i(1-\lambda) \tag{4}$$

where M_i is a system safety margin, given by Eq. (1), and $\mu_i = E[M_i]$ is the mean value of M_i. The parameter λ assumes values in the interval $0 \leq \lambda \leq 1$ and its effect on the system failure probability may be interpreted as a scale factor. The original system is obtained for $\lambda = 1$, and for $\lambda = 0$ the system is highly prone to failure, as the mean value of the system safety margins is $E[M_i(0)] = 0$. For small to intermediate values of λ the increase in the system failure probability is sufficiently high to get accurate estimates of the failure probability by Monte Carlo simulation with moderate computational cost.

As proposed by [12], it is assumed that the failure probability as a function of λ can be written as,

$$p_f(\lambda) \underset{\lambda \to 1}{\approx} q(\lambda)\exp\left\{-a\left(\lambda - b\right)^c\right\} \tag{5}$$

where $q(\lambda)$ is a slowly varying function compared with the exponential function $\exp\{-a(\lambda - b)^c\}$. For practical applications it can be implemented in the following form [12]:

$$p_f(\lambda) \approx q\exp\left\{-a\left(\lambda - b\right)^c\right\} \quad \text{for} \quad \lambda_0 \leq \lambda \leq 1 \tag{6}$$

for a suitable value of λ_0, with the function $q(\lambda)$ replaced by a constant q. An important part of the method is therefore to identify a suitable λ_0 so that Eq. (6) represents a good approximation of $p_f(\lambda)$ for $\lambda \in [\lambda_0, 1]$.

The functional form assumed in Eq. (5) is strictly speaking based on an underlying assumption that the reliability problem has been transferred to normalized Gaussian space where a FORM or SORM (or similar) type of approximation would work for the transformed limit state functions. However, when the basic random variables have 'exponential' type of distributions, like e.g. Weibull, normal, lognormal, Gumbel, there is no need to make a transformation to normalized Gaussian space. One can then instead work in the original space and adopt Eq. (6) there. This is the procedure adopted in this paper.

The practical importance of the approximation provided by Eq. (6) is that the target failure probability $p_f = p_f(1)$ can be obtained from values of $p_f(\lambda)$ for $\lambda < 1$. This is the main concept

of the estimation method proposed in [12], as it is easier to estimate the failure probabilities $p_f(\lambda)$ for $\lambda < 1$ accurately than the target value, since they are larger and hence require less simulations and therefore less computational cost. Fitting the approximating function for $p_f(\lambda)$ given by Eq. (6) to the estimated values of failure probability obtained by Monte Carlo simulation with $\lambda < 1$, will then allow us to provide an estimate of the target failure probability by extrapolation.

It may be noted that the method described above is, in fact, very different from an importance sampling procedure. While importance sampling is very vulnerable to the dimension of the space of basic random variables, this is not at all the case with the method described here [13].

2.1 Monte Carlo based reliability estimation by optimized fitting

To find the four parameters q, a, b and c in Eq. (6) defining the optimal fit between function and estimated values of failure probability obtained by Monte Carlo simulation, an optimized fitting procedure was suggested in [12].

For a sample of size N of the vector of basic random variables $\boldsymbol{X} = [X_1, \ldots, X_n]^T$, let $N_f(\lambda)$ denote the number of samples for which failure of the system is verified. An empirical estimate of the failure probability is then given by,

$$\hat{p}_f(\lambda) = \frac{N_f(\lambda)}{N}. \tag{7}$$

The coefficient of variation of this estimator is,

$$C_v\left(\hat{p}_f(\lambda)\right) = \sqrt{\frac{1-p_f(\lambda)}{p_f(\lambda)N}}, \tag{8}$$

which for small failure probabilities can be approximated by,

$$C_v\left(\hat{p}_f(\lambda)\right) \approx \frac{1}{\sqrt{p_f(\lambda)N}}. \tag{9}$$

A fair approximation of the 95% confidence interval for the value $p_f(\lambda)$ can be obtained as $\mathrm{CI}_{0.95}(\lambda) = [C^-(\lambda), C^+(\lambda)]$, where,

$$C^{\pm}(\lambda) = \hat{p}_f(\lambda)\left[1 \pm 1.96 C_v\left(\hat{p}_f(\lambda)\right)\right]. \tag{10}$$

Considering now that we have obtained empirical estimates of the failure probability using Eq. (7) for a suitable set of λ values, the problem then becomes one of finding the optimal fit between the proposed approximating function for the failure probability given by Eq. (6) and the empirical estimates obtained. As proposed in [12], this optimal fit can be carried out by minimizing the following mean square error function with respect to the four parameters q, a, b and c in Eq. (6) at the log level:

$$F(q,a,b,c) = \sum_{j=1}^{M} w_j \left[\log \hat{p}_f(\lambda_j) - \log q + a\left(\lambda_j - b\right)^c\right]^2 \tag{11}$$

where $\lambda_0 \le \lambda_1 \le \ldots < \lambda_M < 1$ denotes the set of λ values where the failure probability is empirically estimated and w_j denotes a weight factor that puts more emphasis on the more reliable

data points. The choice of the weight factors is to some extent arbitrary. The following definition was suggested in [12]:

$$w_j = \left[\log C^+\left(\lambda_j\right) - \log C^-\left(\lambda_j\right)\right]^{-\theta} \tag{12}$$

with θ = 1 or 2, combined with a Levenberg - Marquardt least squares optimization method. This has proved to work well provided that a reasonable choice of the initial values for the parameters is made. In this study $\theta = 2$ is adopted for the optimized fitting. Note that the definition adopted for w_j puts some restriction on the use of the data. Usually, there is a level λ_j beyond which w_j is no longer defined. Hence, the summation in the mean square error function given by Eq. (12) has to stop before that happens. Also, the data should be preconditioned by establishing the tail marker λ_0 in a sensible way.

Although the Levenberg-Marquardt least squares method as described above generally works well, it may be simplified by exploiting the structure of the mean square error function F. It is realized by scrutinizing Eq. (11) that if b and c are fixed, the optimization problem reduces to a standard weighted linear regression problem. That is, with both b and c fixed, the optimum values of a and $\log q$ are found using closed-form weighted linear regression formulas in terms of w_j, $y_j = \log \hat{p}_f\left(\lambda_j\right)$ and $x_j = \left(\lambda_j - b\right)^c$.

It is obtained that the optimal values of a and q are given by the relations:

$$a^*\left(b,c\right) = -\frac{\sum_{j=1}^{M} w_j\left(x_j - \overline{x}\right)\left(y_j - \overline{y}\right)}{\sum_{j=1}^{M} w_j\left(x_j - \overline{x}\right)^2} \tag{13}$$

and

$$\log q^*\left(b,c\right) = \overline{y} + a^*\left(b,c\right)\overline{x} \tag{14}$$

where

$$\overline{x} = \sum_{j=1}^{M} w_j x_j \Big/ \sum_{j=1}^{M} w_j \tag{15}$$

and

$$\overline{y} = \sum_{j=1}^{M} w_j y_j \Big/ \sum_{j=1}^{M} w_j \tag{16}$$

The Levenberg-Marquardt method may now be used on the function $\tilde{F}\left(b,c\right) = F\left(q^*\left(b,c\right), a^*\left(b,c\right), b, c\right)$ to find the optimal values b^* and c^*, and then the corresponding a^* and q^* can be calculated from Eqs. (13) and (14).

For estimation of the confidence interval for a predicted value of the failure probability provided by the optimal curve, the empirical confidence band given by Eq. (10) is reanchored to the optimal curve. The range of fitted curves that stay within the reanchored confidence band will determine an optimized confidence interval of the predicted value. As a final point, it was verified that the predicted value is not very sensitive to the choice of λ_0 provided that it is chosen with some care.

3 NETWORK ARCH BRIDGE

The concept of network arch bridges has been developed through many years and has been used for road bridges, see [7], as well as train crossings, see [2]. By optimizing the hanger slope configuration of the network the structure can be designed with a significantly lower

mass by steel reduction; over 50 % compared to other similar tie arch bridges with vertical hanger is reported in [17].

Network arch bridges are tied arch bridges with inclined hangers with multiple intersections where the configuration of the tie will follow the arch but with a much larger radius of curvature. This type of arch bridge design is thoroughly described and investigated in several papers by Dr. P. Tveit, e.g. [18]. The inclined hangers are well suited to distribute bending moments and shear forces to the upper and lower chord similar to a truss compared to those in tied arches with vertical hangers where these are relatively large and decisive. Thus, for network arch bridges bending moments in the transverse direction are more important than in the longitudinal direction. This property is one of the main conditions in designing some of the world's most slender bridges.

3.1 Network arch bridge reliability analysis

In the present investigation an enhanced Monte Carlo simulation method is introduced to assess the system buckling reliability of a slender Network arch bridge due to traffic loads. For all slender structures geometric properties are of special interest and their effects on the global system are investigated. Thus, for the presented case study four global imperfections are introduced as basic random variables, width, length, height and the arch out of plumbness. Furthermore, the arch tube member geometric cross section properties are also introduced as random variables. These are the four main steel arch member outer radii's together with corresponding thicknesses. The four arch members are the wind portal frame columns given as the lower part of the arch, wind portal frame girder, wind bracing and the remaining arch members above the wind portal frame, all shown in the Figure 1. These render the 12 basic random variables of the system buckling reliability analysis.

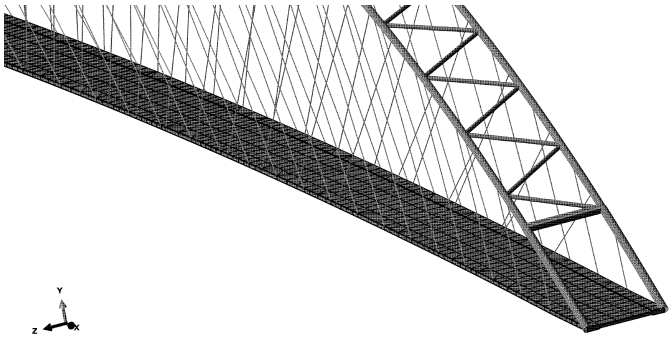

Figure 1. Network arch members with the wind portal frame side columns as part of the arch and top girder as end of the diagonal wind bracing.

All the geometric random variables are assumed uncorrelated normally distributed with the mean values as nominal values (i.e. the dimensions given on drawings). The coefficient of variation (CoV) given in Table 1 are chosen from the guidelines given in [6] with complementation for steel member parameters given in [8].

Random variables	CoV
Tube outer radius, r	2.5 %
Tube thickness, t	2.5 %
Arch length, L	1 / 10.000
Arch height, H	1 / 1000
Arch width, W	1 / 1000
Arch out of plumbness, θ	1.5 $^{o}/_{oo}$

Table 1. Coefficients of variation for basic random variables.

3.2 Model uncertainty

Most civil engineering models are based on an hypothesis of a physical understanding supported by empirical relations between different variables. The engineering models will introduce uncertainties from the inherent physical understanding and the assumed physical model. Incompleteness due to the lack of knowledge and simplifications will give model predictions that differ from real output. This is taken into account in the present analysis by the introduction of a model parameter, *I*, representing the model uncertainties for the load and structural capacity and is treated as a random variable.

A systematic method of choosing and quantify the material and load model uncertainties can be found in the Reliability-Based Classification publication by the Road Directorate, Ministry of Transportation in Denmark [16]. The structural capacity model uncertainty is accounted for by the random variable I_m, introduced by multiplication. This variable is assumed logarithmic normally distributed with a mean value of 1.0 and a coefficient of variation V_{Im}, given by:

$$V_{I_m} = \sqrt{V_{I_1}^{\ 2} + V_{I_2}^{\ 2} + V_{I_3}^{\ 2} + 2\left(\rho_1 V_{I_1} + \rho_2 V_{I_2} + \rho_3 V_{I_3}\right)} \tag{17}$$

Coefficients of variation, V_{Ii}, and correlation coefficients, ρ_i, are determine based on the assumption of three main contributions (i = 1-3). These are the accuracy of the computational mode, uncertainty in determine material parameters and the identity of materials. For the present example selections are made for the structure as a whole. The accuracy of the computational model is assumed normal, uncertainty determining material parameters is set to medium and the identity of materials is assumed normal, rendering $V_i = 0.06$ and $\rho_i = 0.0$ for all three uncertainties.

To quantify the load model uncertainty a similar model can be used [16]. The uncertainty in the computational model for loads are taken into account by introducing a normally distributed stochastic variable, I_f, by addition. The model uncertainty for traffic loading determined from the assumption of medium uncertainty in the loading model can be assumed to have a mean value 0.0 and a coefficient of variation, $V_{If} = 0.15$.

3.3 Traffic load

The Traffic load represents one of the most significant contributions to the total value of the external actions to be considered in the ultimate limit state analysis. In the present reliability analysis is a traffic load model, which represent one of several load cases, sought for a given return period. The traffic loads on bridges will by its nature inherent a great complexity due to the high randomness, thus is difficult to model accurately. This is a natural consequence of the load which varies significantly, also due to its site dependency, especially for long spanning bridges [4].

The uncertainty in the traffic load is dependent on several statistical variables involved describing the problem. Among those which may be considered are the type of vehicle, intervals between vehicles, gross weight of each vehicle, gross weight distribution to axles, spacing

between extreme axles and between any pair of axles, total external length of the vehicle, velocity, daily intensity of vehicles per lane and the density of vehicles over the road, as described in [1]. In most cases there exists no common analytic expression for the total load distribution and correlation coefficients between all these variables.

In [1] it is shown that the traffic load is highly dependent on the type of vehicles as well as their individual load situations. They have identified relations between characteristic load and maximum load effects. It is shown that the axle load distribution, both for loaded as well as unloaded vehicles are skew distributions, assuming that this represents extreme events; they may most likely be assumed to be Gumbel distributed. Furthermore, if a complete description of the different cases is sought then a multimodal distribution must be introduced. Several similar studies are also reported in [4], which show that a detailed description of the traffic load can be modeled by the sum of several assumed independent distributions.

The traffic load extreme values are in the present investigation assumed to be Gumbel distributed where the described load case is assumed representing a uniformly distributed line load. In the design rules given by the Norwegian Public Road Administration (NPRA) it is not clearly stated what the return period of the characteristic traffic load is. However, the Eurocode NS-EN 1991-2 [10] is based on a return period of 1000 years.

The design of the network arch bridge considered in the present investigation is the characteristic design load given by the NPRA used to determine the site specific probabilistic load model for the reliability analysis. By comparison, using the expected distribution of a 250 m queue weight registered in [4], the assumption of Gumbel distribution and a return period equal to 1000 years can an estimate of the mean and standard deviation for the extreme traffic load be fitted. The result from the load distribution estimation gave a mean and standard deviation as m_q= 3.5 N/m and σ_q = 1.1 N/m, respectively. Finally, the Gumbel distribution given by equation 18, where the scale, α, and location, β, parameters relation to the mean, μ, and standard deviation, σ, of the process are given by (as used in [19]):

$$F(x) = \exp\{-\exp[-\beta(x-\alpha)]\} \tag{18}$$

where $\beta = \pi/\sigma\sqrt{6}$ and $\alpha = \mu - 0.57722/\beta$, rendering the scale parameter β = 1.17 and the location parameter α = 3.0.

3.4 Buckling analysis of network arch bridges

Buckling occurs as a small increase in the axial compressive force in the structure causes a sudden outwards displacement as the loading reaches a certain critical level. This may lead to a sudden collapse of the structure without any initial warning. Thus, buckling does not occur as a result of the applied stress reaching a critical level, but rather depends on variations of component dimensions and the overall geometry of the structure.

Shallow arches are more likely to have non-linear pre-buckling behavior with substantial deformation prior to the buckling. This effect needs to be considered and ensured. If classic buckling analysis is used without including these effects might the critical load be incorrectly predict. Thus, it is important to include the pre-loading face with the possibility of any non-linear response, which in the present paper is ensured by the inclusion of bi-linear material strength and geometric stiffness. This will allow for the correct pre-buckling deformation to occur and the correct stiffness to be established. This is to ensure a correct elastic buckling load which is used in the structural reliability analysis. These effects are investigated in [14] and drafted for the in plane buckling but cannot be excluded to be significant also in the out of plane buckling. As stated in [14] may significant pre-buckling deformations, especially for

shallow arches, significantly reduce the buckling resistance and over estimating the buckling load.

For buckling of network arches will the stiffness of the hangers be of special importance and also significantly influence the estimated buckling capacity. Therefore, the hanger configuration will be favorable for network arches compared to tie arches with vertical hangers.

If the network arch tie remains strait the arch will get in-plane buckling modes as can be found from simple columns supported by flexural springs as pointed out by [15]. Simplified solutions may then be found from in-plane arch calculation methods as introduced in both [14] and [15]. However, it can be seen in the present investigation that the out of plane buckling modes can also be expected. In the case of a large network arch bridge with great slenderness may the symmetric as well as the asymmetric modes appear.

In plane buckling modes for network arches was further investigated in [15]. It shows that buckling load for network arches will be dependent on the arch bending stiffness, the number of hangers as well as the arch to hanger angle. However, the bending stiffness and deflection of the tie will have less influence on the global buckling load.

4 THE BRANDANGER NETWORK ARCH BRIDGE, A CASE STUDY

The Brandanger Bridge situated in the western part of Norway is stated to be the world's most slender arch bridge in [18] and [7], see Figure 2.

Figure 2. The Brandanger Bridge opened on the 4th of November 2010.

The design of the bridge was suggested to the Norwegian public road administration in 2004 by dr. P. Tveit and was finally opened on the 4th of November, 2010. In the present case study is an early suggested version of the bridge design used with some further modifications introduced. However, the main description is the same with a length of 220 m, a width of 7.6 m and an arch bow height of 33 m as shown in Figure 3.

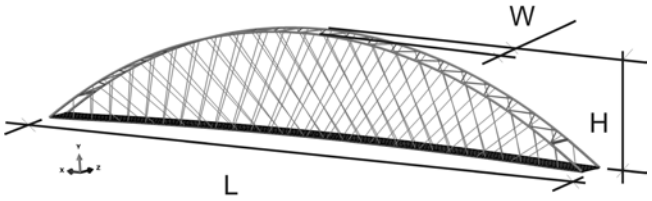

Figure 3. Overall dimensions, width W=7.6m, bow height H=33m and span length L=220m of the network arch bridge.

The bridge consists of a main span with two parallel upper chord steel arches and a lower chord concrete slab tie suspended by 44 hangers on each side. Between the arches is a simple wind portal frame and diagonal wind bracing. The arch as well as the wind bracing consists of steel tube elements, while the inclined hangers are made out of high-strength steel cables. The

bridge deck is constructed by pre-stressed concrete with a total width of just 7.6 meters, creating an extremely light and slender structure. The steel tube profiles of the arch have only some few variations along the arch length. Typically, D·t is 711·40 mm below the wind bracing and 711·35 mm elsewhere. A typical dimension of the concrete slabs is a 250 mm centre thickness, while the first outer 1.1 m on each side has a thickness of 400 mm. below is main material parameters listed.

- Structural steel: density 7850 kg/m3, Young's modulus 210 GPa, yield stress 355 MPa
- Steel hangers: density 7850 kg/m3, Young's modulus 170 GPa, yield stress 1550 MPa
- Concrete bridge deck: density 2200 kg/m3, Young's modulus 28.7 GPa, compressive strength 35 MPa

4.1 Structural response by FE-analysis

The Brandanger Fjord Bridge has in the design stage been subject to extensive numerical analysis such as linear and non-linear static analysis, the prediction of buckling, as well as dynamic time domain analysis. The finite element model for the present analyses is built up of beam elements in the arch with tubular cross sections and the hangers with solid circular cross sections, as well as shell elements for in lower chord bridge deck.

To model the steel network arch in the FE-model are 3-node quadratic Timoshenko beam formulation within Abaqus/Standard used for all arch tube members, wind bracing and wind portal frame girder. For the network hangers is the 2-node linear Timoshenko beam formulation chosen. These beam formulation allows for transverse shear deformation and the beam may be subjected to large axial strains.

The lower chord bridge deck is represented with a simple first order 4-node general purpose conventional shell element with reduced integration formulation within Abaqus/Standard. This element includes thickness changes and transverse shear deformations allowing for large rotations and finite membrane strains.

It is in the FE-analysis procedure distinguishes between general non-linear steps and linear perturbation steps. The general non-linear analysis is defined as sequential events where one state of the model at the end of the step will provide the initial state for the start of the next. The linear perturbation analysis provides the linearized response of the model about the reached state at the end of the last non-linear step. For each step in the analysis can also the procedure account for nonlinear effects from large displacements and deformations. These effects are of special interest in the present buckling investigation, where it is important to account for the pre-buckling deformation.

4.2 Global system buckling reliability estimation

In the present study is a network arch bridge global system buckling limit state function to be evaluated. It includes the derived simplified ultimate traffic load model and the FE linear perturbation eigenvalue solutions of the pre-loaded structure. The system failure is therefore defined as the lowest estimated buckling load exceeding the estimated structural buckling capacity.

Before each evaluation of the system buckling capacity is the system first pre-loaded with the structural self-weight and the nominal traffic load as defined by the Norwegian Public Road Administration design guide Håndbok 185 [5]. This include a uniformly distributed line load of 9 kN/m over a 3 m width and three pairs of point loads, each pair 210 kN, separated by 6 m and 2.5 m. The uniformly distributed traffic load is also introduced as the perturbation load pattern used in the solution. Thus, any pre-load deformation imperfections introduced by

initial loading as well as the geometric stiffness contribution are all established before the buckling analysis.

The reliability of the structure is evaluated by the limit state function defined by the stability failure considered. The bifurcation buckling limit state function can in general terms be stated by:

$$G(\mathbf{X}_R, P_\gamma, I_m, I_f) = P_{cr}(P_B(\mathbf{X}_R), I_m) - P_\gamma\left(P_T(\alpha,\beta), I_f\right) \tag{19}$$

where P_{cr} corresponds to the global system buckling load found by the FE-analysis whereas P_γ is the estimated buckling load estimated from the traffic action. The random variable vector is given by:

$$< \mathbf{X}_R = [t_{arch}, t_{bracing}, t_{port.\,\text{column}}, t_{port.\,girder}, D_{arch}, D_{bracing}, D_{port.\,\text{column}}, D_{por.\,girder}, H, W, L, \theta] \tag{20}$$

The model uncertainty is also introduced by the factors I_m and I_f. The buckling load, P_B, from the FE-analysis is given by the perturbation load and the buckling load factor as:

$$P_B(\mathbf{X}_R) = P_{pert} \cdot \lambda_{cr}(\mathbf{X}_R) \tag{21}$$

whereas the traffic load is estimated from the simplified Gumbel distributed traffic load:

$$P_T = P_T(\alpha,\beta) \tag{22}$$

The remaining structural properties as well as the load distributions are all assumed to be deterministic.

In the present example is the estimated failure probability of the global system buckling event considered. The crude Monte Carlo simulation was used to compute the empirical estimation of failure probability for $\lambda < 1$, as described previously. Each system buckling strength capacity was computed by the bifurcation analysis in Abaqus/Standard with a computational time of approximately 10s on a standard laptop computer, including time to retrieve results and initiate a new analysis. The total number of simulated system buckling analyses was $3.88 \cdot 10^5$ executed in 6 parallel processes, rendering approximately 8 days and nights of computing time. This was deemed as what could be seen as reasonable calculation effort to be invested in the present problem.

Probability of failure for the three first buckling modes are calculated, where the two first are out of plane buckling modes and the third is an in plane buckling mode with significant higher buckling load factor than the first two. Probability of failure is calculated for all three modes using the limit state function in Eq. (19). Typical buckling modes corresponding to the three first modes are shown in Figures 4 – 6.

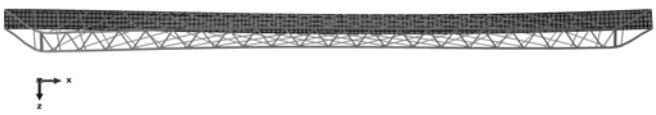

Figure 4. First estimated buckling mode.

Figure 5. Second estimated buckling mode.

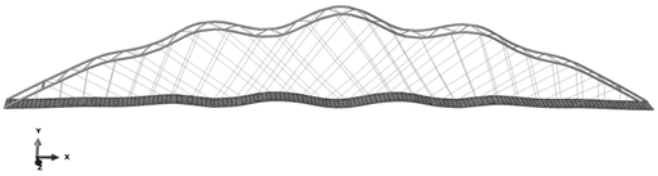

Figure 6. Third estimated buckling mode.

The predicted failure probability and corresponding reliability index at $\lambda = 1$ given by the fitted optimal curves and the re-anchored and optimized 95% confidence interval is given in table 2 and shown in Figures 7-9.

	Pf-	Pf	Pf+	β-	β	β+
M1	4.74·10-7	10.1·10-7	16.9·10-7	4.64	4.75	4.90
M2	1.40·10-7	4.53·10-7	9.66·10-7	4.76	4.91	5.14
M3	0.15·10-9	1.75·10-9	5.01·10-9	5.73	5.91	6.29

Reliability index given by $\beta = -\Phi(P_f)$

Table 2. Network arch bridge probability of failure for global system buckling estimated with the three first buckling modes.

The estimated probabilities of failure comply with expected target probability of failure commonly used in design of civil engineering structures, depending on the consequences of failure and failure modes. In Eurocode NS-EN 1990 [11] are three different target reliabilities in annex B given as 10^{-5}, 10^{-6} and 10^{-7}.

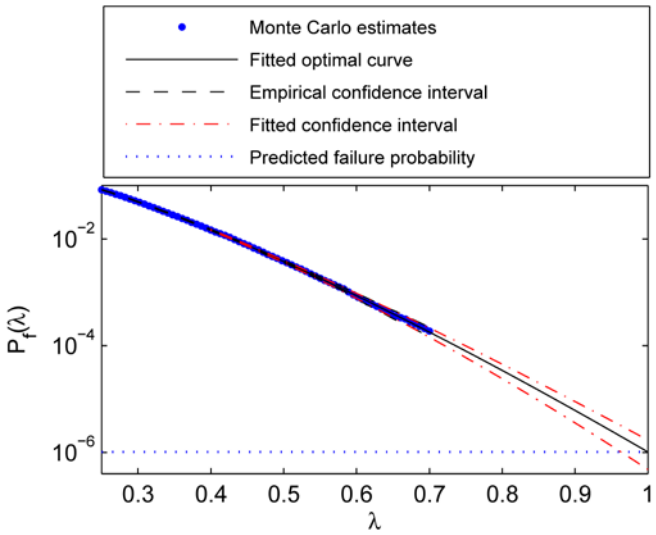

Figure 7. Log plot of failure probability with buckling mode 1. Parameters of the fitted optimal curve: $q = 0.180$, $a = 14.943$, $b = 0.152$ and $c = 1.2825$.

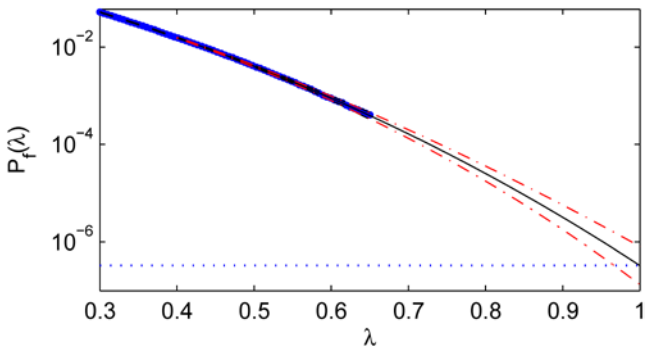

Figure 8. Log plot of failure probability with buckling mode 2. Parameters of the fitted optimal curve: q = 2.452, a = 8.321, b = -0.375 and c = 1.955.

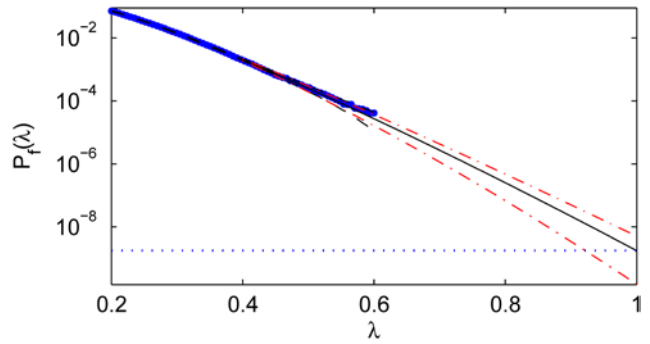

Figure 9. Log plot of failure probability with buckling mode 3. Parameters of the fitted optimal curve: q = 0.087, a = 22.448, b = 0.183 and c = 1.170.

5 CONCLUSIONS

In the present investigation of the global system buckling of a network arch bridge is an efficient enhanced Monte Carlo based method presented to assess the structural reliability. It has been shown that the method provides good estimations of the reliability of the structural global system with a reasonable computational effort. The method is in the study used to estimate the global system buckling failure probability represented by non-linear pre-loaded geometric stiffness and linearized buckling solved by the FE-software Abaqus/Standard. The low values of probability of failure are in agreement with the target values in design codes whit a failure event without warning and with large consequences commonly the set to 10-7. The enhanced Monte Carlo method has shown to be an efficient technique to reduce the necessary number of simulation needed to reach acceptable levels of uncertainty of the estimated reliability index.

6 REFERENCES

REFERENCES

[1] Bez, R. & Bailey, S. 1993. Traffic load models for bridge evaluation: *Second international conference on bridge management*: Surrey, 9 pps

[2] Brunn, B., Schanack, F. & Steinmann, U. 2004, Network arches for railway bridges, *Advvances in Assessment, Structural Design and Construction. CIMNE*, Barcelona

[3] Faber, M.H., 2001. Reliability of Exceptional Structures. World *Congress Safety of Modern Technical Systems*, Cologne Germany,

[4] Getachew, A. 2003. Traffic load effects on bridges, statistical analysis of collected and Monte Carlo simulated vehicle data: *Doctoral thesis at KTH-Stockholm*, 162pps.

[5] Håndbok 185 2009. Bruprosjektering: *Norwegian Public Road Administration*: ISBN 82-7207-591-1, pps. 302

[6] JCSS, 2001. Probabilistic Model Code - Part 1 -3: *Joint Committee on Structural Safety*, ISBN 978-3-909386-79-6

[7] Larsen, R. & Aas-Jakobsen, K. 2006. Brandangersundet Bru – verdens slankeste?: *Nyheter om stål No. 3*. ISSN 1404-9414

[8] Li, K. & Sun, K. 2011. Stochastic parameters analyze for steel highway bridge members: *Geotechnical special publication No. 219GSP, ASCE*: 184-189

[9] Melchers, R.E., 1999, *Structural Reliability Analysis and Prediction*, 2nd Edition, John Wiley & Sons Ltd, Chichester, UK.

[10] NS-EN1991-1-2:2003+NA:2010, Eurocode 1: Actions on Structures - Part 2: Traffic loads on bridges

[11] NS-EN1990:2002+NA:2008, Eurocode : Basis of structural design

[12] Naess, A., Leira, B.J. and Batsevych, O., 2009, System Reliability Analysis by Enhanced Monte Carlo Simulation, *Structural Safety*, Vol. **31**, pp. 349-355.

[13] Naess, A., Leira, B.J. and Batsevych, O., 2010, Efficient Reliability Analysis of Structural Systems with a High Number of Limit States, *Proceedings of the 29th International Conference on Offshore Mechanics and Artic Engineering* (OMAE2010), June 6-11, Shanghai, China.

[14] Pi, Y. L. & Bradford, B. U. 2002. In-plane stability of arches, *International journal of solids and structures*: 105-125

[15] Schanack, F. 2009. Berechnung der Knicklast in Bogenebene von Netzwerkbögen: *Bautechnik* Vol 86, Issue 5 p. 249-255

[16] Scholten, C.v., Enevoldsen, I., Arnbjerg-Nielsen, T., Randrup-Thomsen, S., Sloth, M. & Engelund, S., (2004). *Reliability-Based Classification of the Load Carrying Capacity of Existing Bridges* Road Directorate - Ministry of Transport Denmark, ISBN 87-7923-774-6

[17] Tveit, P. 2006. Optimal network arches for coastal regions: *International conference on bridges*: Dubrovnik pp. 721-728

[18] Tveit, P. 2011. The Network Arch. Bits of Manuscript in February 2011 after Lectures in 50 Countries Internet edition, Grimstad,
way ://home.uia.no/pert/index.php/Home

[19] Xiangyang, W. & Guanghui, Z. 2010. Bridge reliability analysis based on the FEM and Monte Carlo method: *International conference on intelligent computation technology and automation*, Changsha, China: 891-894.